Sigma 1 Receptor Contributes to Astrocyte-Mediated Retinal Ganglion Cell Protection

Jing Zhao,[1,3] Graydon B. Gonsalvez,[2] Barbara A. Mysona,[1–3] Sylvia B. Smith,[1–3] and Kathryn E. Bollinger[1–3]

[1]Department of Ophthalmology, Medical College of Georgia at Augusta University, Augusta, Georgia, United States
[2]Department of Cellular Biology and Anatomy, Augusta, Georgia, United States
[3]Culver Vision Discovery Institute, Augusta, Georgia, United States

Correspondence: Kathryn E. Bollinger, Associate Professor of Ophthalmology, Cellular Biology and Anatomy, 1120 15th St BA 2701, Augusta, GA 30912, USA; kbollinger@augusta.edu.

Received: October 31, 2021
Accepted: December 28, 2021
Published: February 1, 2022

Citation: Zhao J, Gonsalvez GB, Mysona BA, Smith SB, Bollinger KE. Sigma 1 receptor contributes to astrocyte-mediated retinal ganglion cell protection. *Invest Ophthalmol Vis Sci.* 2022;63(2):1. https://doi.org/10.1167/iovs.63.2.1

Purpose. Sigma 1 receptor (S1R) is expressed in retinal ganglion cells (RGCs) and astrocytes, and its activation is neuroprotective. We evaluated the contribution of S1R within optic nerve head astrocytes (ONHAs) to growth and survival of RGCs in vitro.

Methods. Wild-type (WT) RGCs and WT or S1R knockout (S1R KO) ONHAs were cocultured for 2, 4, or 7 days. Total and maximal neurite length, neurite root, and extremity counts were measured. Cell death was measured using a TUNEL assay. Signal transducer and activator of transcription 3 phosphorylation levels were evaluated in ONHA-derived lysates by immunoblotting.

Results. The coculture of WT RGCs with WT or S1R KO ONHAs increased the total and maximal neurite length. Neurite root and extremity counts increased at 4 and 7 days when WT RGCs were cocultured with WT or S1R KO ONHAs. At all timepoints, the total and maximal neurite length decreased for WT RGCs in coculture with S1R KO ONHAs compared with WT ONHAs. Root and extremity counts decreased for WT RGCs in coculture with S1R KO ONHAs compared with WT ONHAs at 2 and 7, but not 4 days. RGC apoptosis increased in S1R KO ONHA coculture and S1R KO-conditioned medium, compared with WT ONHA coculture or WT-conditioned medium. S1R KO ONHA-derived lysates showed decreased phosphorylated signal transducer and activator of transcription 3 levels compared with WT ONHA-derived lysates.

Conclusions. The absence of S1R within ONHAs has a deleterious effect on RGC neurite growth and RGC survival, reflected in analysis of WT RGC + S1R KO ONHA indirect cocultures. The data suggest that S1R may enhance ganglion cell survival via glia-mediated mechanisms.

Keywords: optic nerve head astrocyte, retinal ganglion cells, neuroprotection

Sigma 1 receptor (S1R) is a small (25.3 kDa), unique, transmembrane protein that is enriched within the endoplasmic reticulum.[1,2] S1R functions to modulate multiple intracellular signaling and cell survival pathways through a variety of mechanisms that are not fully understood.[3–7] Importantly, S1R is expressed in both neuronal and glial cell types throughout the central and peripheral nervous systems, including the optic nerve head.[8–11] Within the eye, studies indicate that targeting S1R is beneficial in optic nerve and retinal disorders that affect ganglion cells and photoreceptors.[12–17] For example, retinal ganglion cell (RGC) loss was attenuated and retinal structure preserved by administration of the S1R agonist (+)-pentazocine ((+)-(PTZ)) in rodent models of diabetic retinopathy and NMDA-induced inner retinal toxicity.[18,19] Furthermore, investigations of S1R knockout (S1R KO) animals indicate that loss of S1R leads to accelerated neurodegenerative pathology in the brain, spinal cord, and optic nerve.[20–25]

In addition to in vivo investigations, in vitro studies have shown that S1R activation can protect isolated primary RGC cultures from apoptosis under conditions of excitotoxic and oxidative stress.[13,14,26] Furthermore, our recent studies using primary cultures of optic nerve head-derived astrocytes (ONHAs) show that stimulation of S1R using (+)-PTZ mitigates the generation of intracellular reactive oxygen species and protects against astrocyte cell death.[27] Whether S1R within ONHAs can function to protect RGCs independent of S1R activation within the RGCs themselves is an unknown but critically important question.

Astrocytes throughout the central nervous system (CNS) have both neuroprotective and neurotoxic properties, and these characteristics depend on contextual and environmental factors.[28,29] For example, reactivity responses associated with ischemia (stroke), traumatic injury, or neurodegenerative disease show variation at different stages of the same disorder and among astrocyte cohorts derived from different CNS regions.[28,30–32] In vivo studies performed specifically in the ON and ONH under glaucomatous conditions are consistent with the CNS paradigm of disorder and context-specific astrocytic stress

responses.[33–37] In addition, in vitro studies of astrocyte-neuronal cocultures indicate that astrocytes derived from the brain frontal cortex region can robustly protect RGCs from apoptosis, but that astrocytes derived from the optic nerve region may only weakly promote RGC survival.[38,39] However, few studies have examined RGC–ONHA interactions in controlled, ex vivo environments.

Here, we report use of an in vitro, indirect coculture system of primary RGCs and primary ONHAs. We observe a clear increase in viability when RGCs are cocultured with adult, murine-derived ONHAs. Using the ONHA–RGC coculture system, we evaluate the extent to which lack of S1R in ONHAs alters RGC neurite growth and survival compared with WT ONHAs. We find that, compared with WT-derived ONHAs, S1R knockout (KO)-derived ONHAs are significantly less protective of WT RGCs in coculture. These results suggest that, in vitro, S1R may provide neuroprotection through glia-mediated mechanisms.

Methods and Materials

Animals

Experiments requiring animals adhered to the ARVO Statement for the Use of Animals in Ophthalmic and Vision Research. Our animal protocol is approved by Augusta University Institutional Animal Care and Use Committee (IACUC, 2011-0338). C57BL/6J (WT) mice (The Jackson Laboratory, Bar Harbor, ME) and S1R KO mice (see Wang et al.[40]) were kept under controlled lighting conditions (12-h light: 12-h dark).

Primary Mouse Optic Nerve Head Astrocytes (ONHAs) Culture

Primary mouse ONHAs were isolated from optic nerve head of WT mice and S1R KO mice according to our previously published protocol.[41] Briefly, 6-week-old mice were euthanized. Six mice were used for each ONHA isolation and cell culture experiment. Optic nerve head tissue was dissected proximal to the sclera and was digested for 15 minutes using 0.05% trypsin (Invitrogen, Carlsbad, CA) at 37 °C. Cells were washed once with ONHA growth media (Dulbecco's modified Eagle's medium/F12; Invitrogen) containing 10% of fetal bovine serum (Atlanta Biologicals, Atlanta, GA), 1% penicillin/streptomycin (Invitrogen), 1% Glutamax (Invitrogen), and 25 ng/mL epidermal growth factor (Sigma, St. Louis, MO), and spun for 5 minutes at 2000 rpm. Cells were resuspended in ONHA growth media and plated on 0.2% gelatin (Sigma) coated T75 cell-culture flasks. Cells were maintained in a humidified incubator containing 5% CO_2 at 37°C. Cells were passaged after 7 to 10 days and were used at passages two through five. Immunocytochemistry was used to verify the purity of ONHA cultures and results are shown in Supplementary Figure S1.

Isolation and Culture of Primary RGCs

Primary RGCs were prepared from 3- to 5-day-old WT mouse retinas according to the method by Dun et al.[42] and Winzeler et al.[43] with modifications. Briefly, 16 to 24 retinas were incubated for 15 minutes at 37 °C in papain buffer (16.5 U/mL papain; Worthington Biochemical Corp., Lakewood, NJ) and 0.2 mg/mL L-cysteine (Sigma). Tissue was triturated in DPBS containing 0.15% trypsin inhibitor (Worthington), 0.15% BSA (Sigma), 0.04% DNase (Sigma), and rabbit anti-macrophage antiserum (Accurate Chemical & Scientific Corp, Carle Place, NY), and incubated at room temperature for 15 minutes. Resulting cells were pelleted by centrifugation (5 minutes, 2000 rpm) and then resuspended in DPBS containing 1% trypsin inhibitor and 1% BSA. The cell suspension was centrifuged (5 minutes, 2000 rpm) and the pellet was resuspended in panning buffer (DPBS, 0.02% BSA, 5 µg/mL insulin [Sigma], 60 µg/mL *N*-acetyl-L-cysteine [Sigma]). The cell suspension was incubated in a 75 cm^2 flask precoated with AffiniPure donkey anti-rabbit IgG (H+L) antibody (Jackson ImmunoResearch, West Grove, PA) at room temperature for 1 hour to remove macrophages and microglial cells. Nonadherent cells were incubated on a 100-mm Petri dish precoated with AffiniPure donkey anti-rat IgG (H+L) antibody (Jackson ImmunoResearch) conjugated to rat anti-mouse Thy-1.2 antibody (BD Biosciences, Franklin Lakes, NJ) at room temperature for 1 hour. Adherent RGCs were released by incubation with 0.125% trypsin (Sigma) in EBSS at 37°C for 5 minutes, followed by the addition of 30% fetal bovine serum in neurobasal medium (Thermo Fisher Scientific, Waltham, MA). The suspension of RGCs was collected by centrifugation (5 minutes, 2000 rpm). The pellet was resuspended in neurobasal medium containing 5 µg/mL insulin (Sigma), 1 mM sodium pyruvate (Thermo Fisher Scientific), 0.1 mg/mL transferrin (Sigma), 60 ng/mL progesterone (Sigma), 16 µg/mL putrescine (Sigma), 40 ng/mL sodium selenite (Sigma), 40 ng/mL tri-iodo-thyronine (Sigma), 1 mM L-glutamine (Thermo Fisher Scientific), 60 µg/mL *N*-acetyl cysteine (Sigma), 2% B27 (Thermo Fisher Scientific), 50 ng/mL brain-derived neurotrophic factor (Sigma), 10 ng/mL CNTF (Sigma), 10 ng/mL forskolin (Sigma), 10 ng/mL basic fibroblast growth factor (Sigma), 0.1 mg/mL BSA. Cells were plated on coverslips coated with poly-D-lysine (Sigma) and laminin (ThermoFisher). One-half of the culture medium was changed every other day.

Coculture of Primary RGCs With Primary ONHAs

The RGC/ONHA indirect coculture system was established based on the protocol by Navneet et al.[44] with minor modifications. Briefly, 1 day before RGC isolation, WT or S1R KO OHNAs were seeded on a 0.4-µm pore size cell culture insert (ThermoFisher) at a density of 25,000 cells per insert. RGCs were isolated by a two-step immunopanning procedure from WT mice as described elsewhere in this article. After 1 hour of seeding RGCs on coverslips, ONHAs inserts were placed within the wells containing RGCs (Fig. 1A). In this coculture system, RGCs and ONHAs were cultured in the RGCs culture medium as described elsewhere in this article.

Immunocytochemistry

After 2, 4, and 7 days, RGCs on coverslips were fixed with 4% paraformaldehyde (Electron Microscopy Sciences, Hatfield, PA) at room temperature for 15 minutes, followed by washing three times with PBS. Cells were then membrane permeabilized with 0.3% triton X-100 in PBS at room temperature for 10 minutes. Next, cells were blocked with 0.1% triton X-100 in PBS with 10% goat serum (Sigma) at room temperature for 1 hour, then incubated in βIII-tubulin antibody (1:500, Abcam, Cambridge, MA) at 4 °C overnight. Next, cells were incubated in secondary antibody (Alexa Fluor

Investigative Ophthalmology & Visual Science

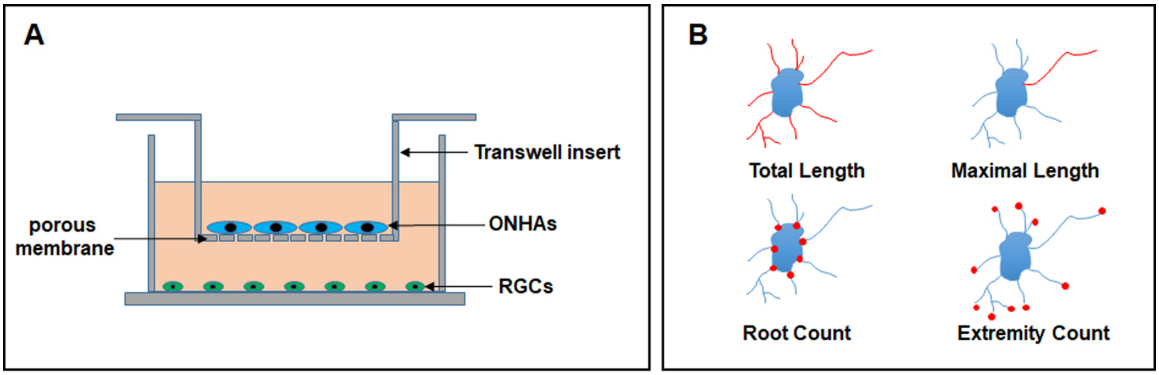

Figure 1. Coculture and neurite outgrowth measurements. (**A**) Coculture model of RGCs and ONHAs. Porous membrane transwell inserts (0.4 µm pore size) separated the culture system into two chambers. The RGCs were placed on the bottom of the lower chamber, and the ONHAs were placed on the membrane of the upper chamber. (**B**) Illustration of neurite outgrowth evaluation for total length, maximal length, root and extremity counts.

555-labeled goat anti rabbit 1:1000; Invitrogen) at room temperature for 2 hours. After washing three times with 0.1% triton X-100 in PBS, coverslips were mounted with Fluoroshield with DAPI (Sigma). Cells were observed for immunofluorescence using a Zeiss Axio Imager D2 microscope (Carl Zeiss, Oberkochen, Germany) equipped with Zeiss Zen23pro software and a high-resolution camera. RGCs neurites were traced and evaluated using the Simple Neurite Tracer plugin within ImageJ software.[45]

Western Blot Analysis

Mouse ONHAs were lysed in RIPA buffer (Sigma, St. Louis, MO) containing 2 mM sodium orthovanadate and 1% protease inhibitor cocktail (Thermo Fisher Scientific). Cell lysates were centrifuged at 14,000 g for 30 minutes. Protein concentration was measured by Bradford assay (Bio-Rad, Hercules, CA). Proteins were separated by electrophoresis on a 4% to 15% SDS-polyacrylamide gel (BioRad) and then transferred to a nitrocellulose membrane (Thermo Fisher Scientific). The membrane was blocked with 5% nonfat milk in Tris-buffered saline-0.05% Tween 20 for 1 hour at room temperature, then incubated overnight at 4°C with primary antibodies (pSTAT3 1:500 [Cell Signaling, Danvers, MA]; STAT3 1:500 [Cell Signaling]; S1R 1:500). After three washes in Tris-buffered saline-0.05% Tween 2, the membrane was incubated for 1 h with an appropriate horseradish peroxidase–conjugated secondary antibody (Santa Cruz Biotechnology, Dallas, TX) at room temperature. Proteins were visualized by incubating with a SuperSignal West Pico chemiluminescent substrate (Thermo Fisher Scientific) and quantified by densitometry with ImageJ software (http://imagej.nih.gov/ij/) provided in the public domain by the National Institutes of Health (Bethesda, MD). The S1R rabbit polyclonal antibody was raised from peptide sequence SEVYYPGETVVHGPGEATDVEWG (corresponds with residues 143–165 of rat S1R) and generated within the laboratory of Dr Sylvia Smith. This antibody has been used in numerous publications since 2002 as a tool for study of S1R expression and function.[46]

TUNEL Assay

After mouse RGCs were cultured on coverslips for 7 days, TUNEL analysis (ApopTag Fluorescein In Situ Apoptosis Detection Kit) was performed per the manufacturer's instructions. The coverslips were mounted with Fluoroshield with DAPI (Sigma). The number of cells emitting the green fluorescence indicating apoptosis were counted. Data are expressed as apoptotic cells per total number of cells in the field (nuclei visualized by DAPI).

Statistical Analysis

Data were analyzed by one-way ANOVA followed by Tukey-Kramer post hoc test for multiple comparisons. Significance was set at a P value of less than 0.05 (Prism; GraphPad Software, Inc. La Jolla, CA).

Results

Our previous in vitro studies have shown that activation of S1R enhances ONHA reactivity characteristics.[41] To evaluate the effects of ONHAs, which express S1R versus those that do not, on RGCs in vitro, we adapted an indirect coculture method as previously described for combined culture of Müller cells with RGCs (Fig. 1A).[44] The present studies used primary RGCs isolated from postnatal WT C57BL6 mice and primary ONHAs isolated from adult WT C57BL6 and S1R KO mice. Under indirect ONHA/RGC coculture conditions, we evaluated RGC neurite outgrowth and survival. To evaluate features of RGC morphology in coculture, we performed quantitative analysis of total and maximal neurite length as well as neurite root and extremity count (Fig. 1B).

To compare measures of RGC health in the presence and absence of ONHAs that either expressed S1R or did not, we performed a primary RGC culture alone and using the indirect ONHA/RGC coculture system. The ONHAs for indirect coculture were harvested from WT or S1R KO mice (Fig. 1A).[44] After 2, 4, and 7 days, we measured neurite outgrowth parameters as described in the Methods.

Two days after seeding, comparison between groups revealed a significant increase in both total and maximal neurite length when WT RGCs were cocultured with either WT ONHAs or S1R KO ONHAs compared with WT RGC culture alone (Figs. 2A–D). A further analysis of the measurements showed a significant decrease in both total and maximal neurite length for WT RGCs cocultured with S1R

Investigative Ophthalmology & Visual Science

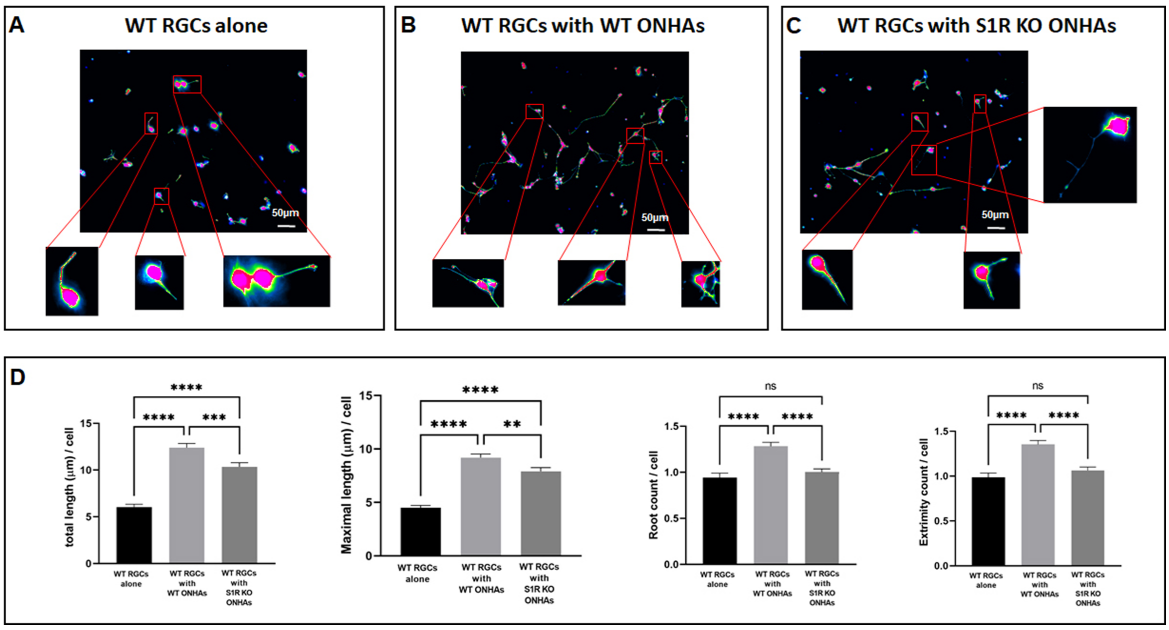

Figure 2. RGC neurite outgrowth after 2 days. WT RGCs were isolated from neonatal mouse pups and cultured for 2 days. Scale bar, 50 µm. (**A**) WT RGCs were plated alone on coverslips in the lower coculture chamber. (**B**) WT RGCs were plated on coverslips in the lower coculture chamber, and WT ONHAs were seeded on the membrane of the upper coculture chamber. (**C**) WT RGCs were plated on coverslips in the lower coculture chamber, and S1R KO ONHAs were seeded on the membrane of the upper coculture chamber. (**D**) RGC neurites were traced using Image J, Simple Neurite Tracer function, with green-colored overlay reflecting traced neurites. The total and maximal neurite length were measured and root and extremity numbers were counted. Significantly different from control at $^{**}P < 0.01$, $^{****}P < 0.0001$. Data were analyzed using one-way ANOVA followed by the Tukey-Kramer post hoc test for multiple comparisons. Two coverslips, and eight microscopic fields per coverslip were quantified from each group of each isolation. The total number of cells analyzed per group was $N = 200–350$. The experiments were repeated in triplicate with cells isolated from different dates, different animals.

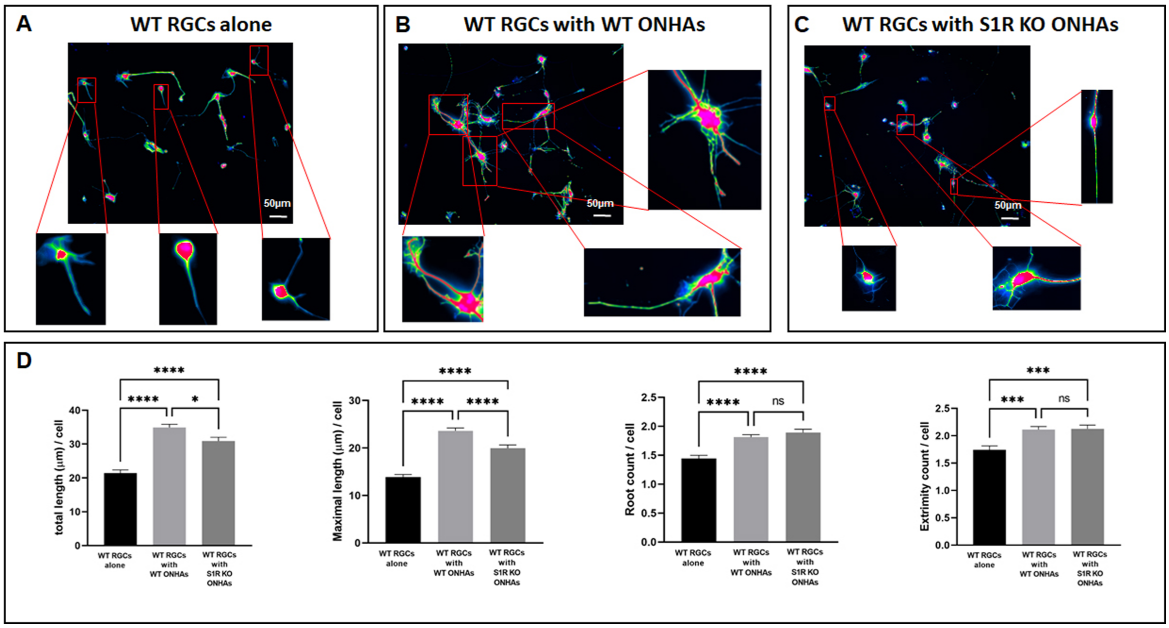

Figure 3. RGC neurite outgrowth after 4 days. WT RGCs were isolated from neonatal mouse pups and cultured for 4 days. Scale bar, 50 µm. (**A**) WT RGCs plated alone on coverslips. (**B**) WT RGCs were plated on coverslips in the lower chamber and WT ONHAs were seeded on the membrane of the upper coculture chamber. (**C**) WT RGCs were plated on coverslips in the lower coculture chamber, and S1R KO ONHAs were seeded on the membrane of the upper chamber. (**D**) RGC neurites were traced using Image J, Simple Neurite Tracer function, with green-colored overlay reflecting traced neurites. The total and maximal neurite length were measured and root and extremity numbers were counted. Significantly different from control at $^{*}P < 0.05$, $^{**}P < 0.01$, $^{***}P < 0.001$, $^{****}P < 0.0001$. Data were analyzed using one-way ANOVA followed by the Tukey-Kramer post hoc test for multiple comparisons. Two coverslips, and eight microscopic fields per coverslip, were quantified from each group of each isolation. The total number of cells analyzed per group was $N = 150–400$. The experiments were repeated in triplicate with cells isolated from different dates, different animals.

Investigative Ophthalmology & Visual Science

KO ONHAs compared with WT RGCs cocultured with WT ONHAs. (Figs. 2B–D). Quantification of neurite root and extremity counts was then performed (Fig. 2D). This analysis revealed significantly increased root and extremity counts when WT RGCs were cocultured with WT ONHAs, compared with WT RGC culture alone. In addition, there was a trend toward increased root and extremity counts when WT RGCs were cocultured with S1R KO ONHAs, compared with WT RGC culture alone (Fig. 2D). However, this trend was not significant. A further analysis of measurements showed a significant decrease in root and extremity counts when WT RGCs were cocultured with S1R KO ONHAs compared with coculture with WT ONHAs (Fig. 2D).

Four days after seeding, neurite outgrowth was evaluated in RGCs alone versus in coculture with WT or S1R KO ONHAs (Figs. 3A–D). An analysis of RGC morphology parameters revealed a significant increase in both total and maximal neurite length when WT RGCs were cocultured with either WT or S1R KO ONHAs compared with WT RGC culture alone (Figs. 3A–D). Further analysis showed a significant decrease in both total and maximal neurite length for WT RGCs cocultured with S1R KO ONHAs compared with WT RGCs cocultured with WT ONHAs. (Fig. 3D). Quantification of neurite root and extremity counts showed a significant increase in both parameters when WT RGCs were cocultured with either WT or S1R KO ONHAs compared with WT RGC culture alone. Finally, a comparison after 4 days showed no significant difference in root or extremity counts between WT RGCs cocultured with S1R KO ONHAs versus WT RGCs cocultured with WT ONHAs. (Fig. 3D).

Next, we evaluated the WT RGC neurite outgrowth after 7 days in culture. An assessment of RGC morphology parameters revealed a significant increase in both total and maximal neurite length when WT RGCs were cocultured with either WT ONHAs or S1R KO ONHAs compared with WT RGC culture alone (Figs. 4A–D). Additional analysis showed a significant decrease in both total and maximal neurite lengths when WT RGCs were cocultured with S1R KO ONHAs compared with WT RGCs cocultured with WT ONHAs. Next, quantification of neurite root and extremity count showed a significant increase in both parameters when WT RGCs were cocultured with either WT ONHAs or S1R KO ONHAs compared with WT RGC culture alone (Fig. 4D). Furthermore, an analysis of measurements showed a significant decrease in both root and extremity counts in WT RGCs cocultured with KO ONHAs compared with WT RGCs cocultured with WT ONHAs. (Fig. 4D).

To compare RGC neurite outgrowth over the time period studied, the complete data shown in Figures 2 through 4, were then analyzed. The values for RGC neurite total and maximal length, root and extremity counts were all compared over 2, 4, and 7 days in culture (Fig. 5). This analysis indicated that, across multiple timepoints, indirect coculture of RGCs with either WT or S1R KO ONHAs led to an improvement in measures of RGC neurite extension and complexity compared with RGC culture alone (Fig. 5). In addition, Figures 5A and B illustrate a steady increase in the total and maximal RGC neurite lengths for WT RGCs in coculture with WT ONHAs compared with S1R KO ONHAs or WT RGCs alone.

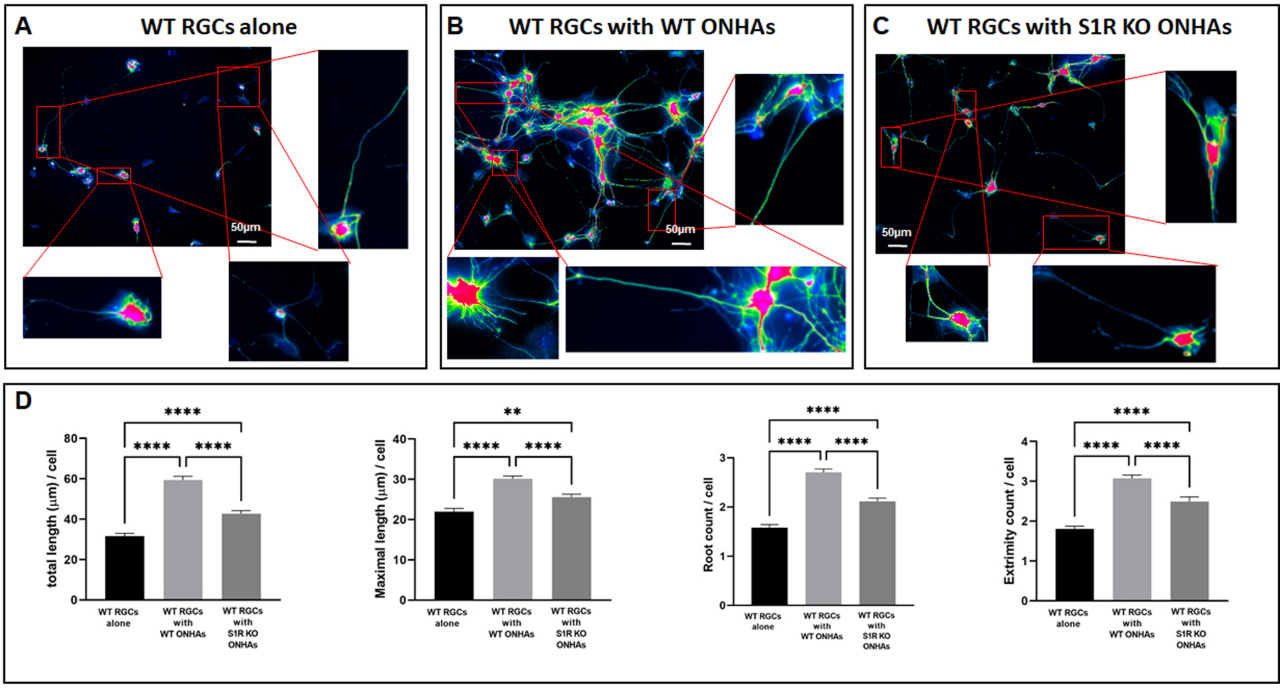

Figure 4. RGC neurite outgrowth after 7 days. WT RGCs were isolated from neonatal mouse pups and cultured for 7 days. Scale bar, 50 µm. (**A**) WT RGCs alone were plated on the coverslips. (**B**) WT RGCs on coverslips were placed on the bottom of the lower chamber, and WT ONHAs were seeded on the membrane of the upper chamber. (**C**) WT RGCs on coverslips were placed on the bottom of the lower chamber, and S1R KO ONHAs were seeded on the membrane of the upper chamber. (**D**) RGC neurites were traced using Image J, Simple Neurite Tracer function, with green-colored overlay reflecting traced neurites. The total and maximal neurite length were measured and root and extremity numbers were counted. Significantly different from control $^{*}P < 0.05$, $^{**}P < 0.01$, $^{****}P < 0.0001$. Data were analyzed using one-way ANOVA followed by Tukey-Kramer post hoc test for multiple comparisons. Two coverslips, and eight microscopic fields per coverslip were quantified from each group of each isolation. The total number of cells analyzed per group was $N = 120–380$. These experiments were repeated in triplicate with cells isolated from different dates, different animals.

Investigative Ophthalmology & Visual Science

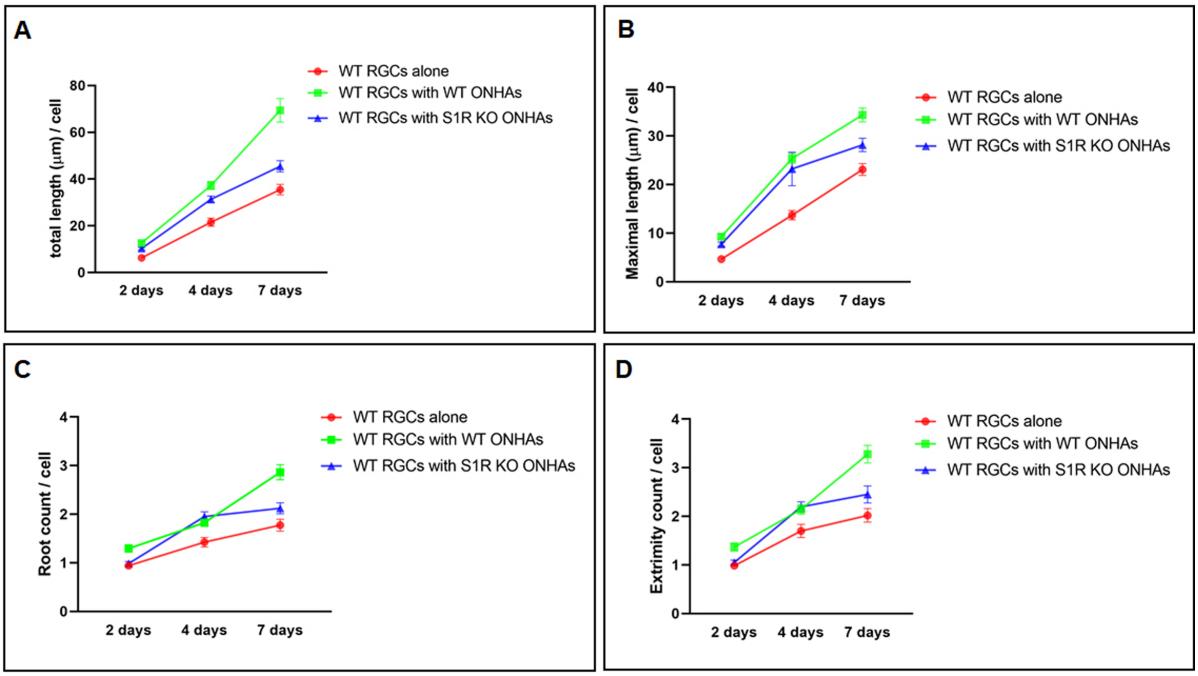

Figure 5. Comparison of neurite outgrowth over time among groups of WT RGCs, alone or in coculture with WT or S1R KO ONHAs. (**A**) Total neurite length measurement. (**B**) The maximal neurite length measurement. (**C**) The root count. (**D**) The extremity count. The experiments analyzed were repeated in triplicate with cells isolated from different dates, different animals.

Furthermore, in Figures 5C and D, the significant increase in RGC neurite root and extremity counts in coculture with either WT or S1R KO ONHAs is obvious after 4 days in culture. The further increase in root and extremity counts in WT RGCs cocultured with WT ONHAs becomes even larger after 7 days in culture compared with either coculture with S1R KO ONHAs or WT RGCs alone (Figs. 5 C and D)

To evaluate whether indirect coculture of ONHAs that expressed S1R or not altered RGC survival, we performed further ONHA/RGC coculture experiments. TUNEL assay was used to evaluate apoptosis of RGCs at the 7-day coculture time-point (Fig. 6A). Quantification of TUNEL-positive cells showed a significant decrease in cellular apoptosis when WT RGCs were cocultured with either WT or S1R KO ONHAs, compared with WT RGCs alone (Fig. 6B). Further comparison between groups showed a significant increase in TUNEL positivity when RGCs were cultured with S1R KO ONHAs compared with WT ONHAs (Fig. 6B). This finding indicates that a lack of S1R within ONHAs leads to decreased protection against WT RGC apoptosis in ONHA/RGC coculture.

To test whether conditioned medium alone derived from ONHAs, with or without S1R, was protective against RGC apoptosis, we cultured isolated WT RGCs for 7 days with regular whole growth medium or with conditioned medium derived from WT ONHAs or S1R KO ONHAs. The day before WT RGCs isolation, WT and S1R KO ONHA were placed in RGC whole growth medium, and the media was

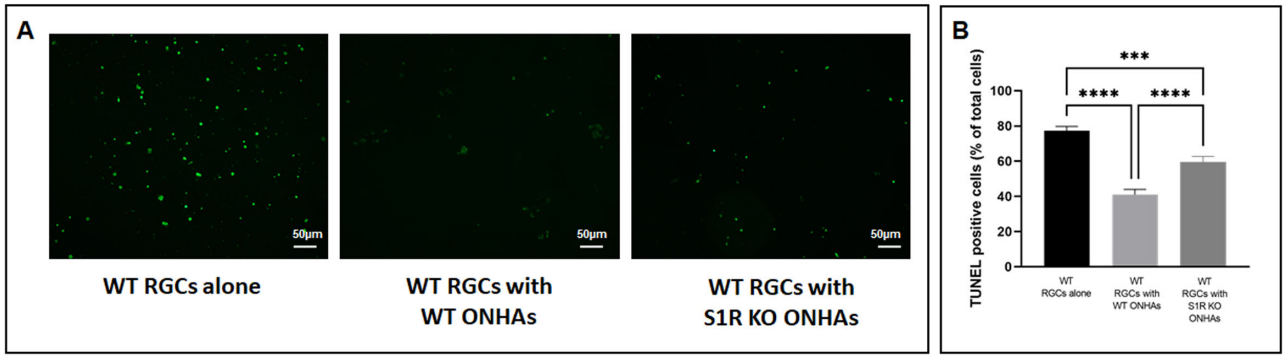

Figure 6. RGC apoptosis alone and in coculture with ONHAs. (**A**) Representative images of TUNEL assay for RGCs alone and in coculture with WT and S1R KO ONHAs. (**B**) Quantification of TUNEL-positive cells. Significantly different from control at $*P < 0.05$, $****P < 0.0001$. Data were analyzed using one-way ANOVA followed by the Tukey-Kramer post hoc test for multiple comparisons. Two coverslips, and eight microscopic fields per coverslip were quantified from each group of each isolation. The total number of cells analyzed was $N = 1000–3000$. These experiments were repeated in triplicate with cells isolated from different dates, different animals.

Investigative Ophthalmology & Visual Science

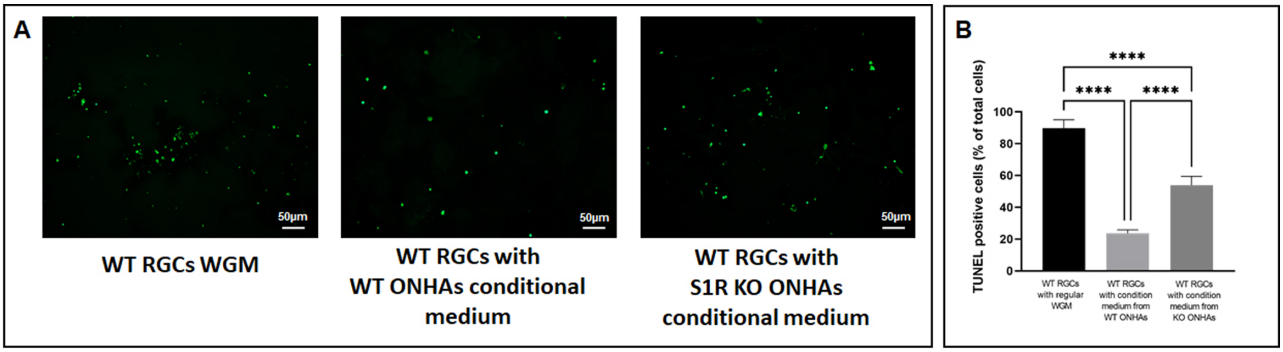

Figure 7. RGC apoptosis alone and with conditioned media. WT RGCs were isolated from neonatal mouse pups and cultured for 7 days with regular whole growth medium or with conditional medium from WT or S1R KO ONHAs. Scale bar, 50 µm. (**A**) Representative images from TUNEL assay. (**B**) Quantification of TUNEL-positive cells. Significantly different from control at ***$P < 0.001$, ****$P < 0.0001$. Data were analyzed using one-way ANOVA followed by the Tukey-Kramer post hoc test for multiple comparisons. Two coverslips, and eight microscopic fields per coverslip were quantified from each group of each isolation. The total number of cells analyzed was $N = 400–2100$. Data are from two isolations.

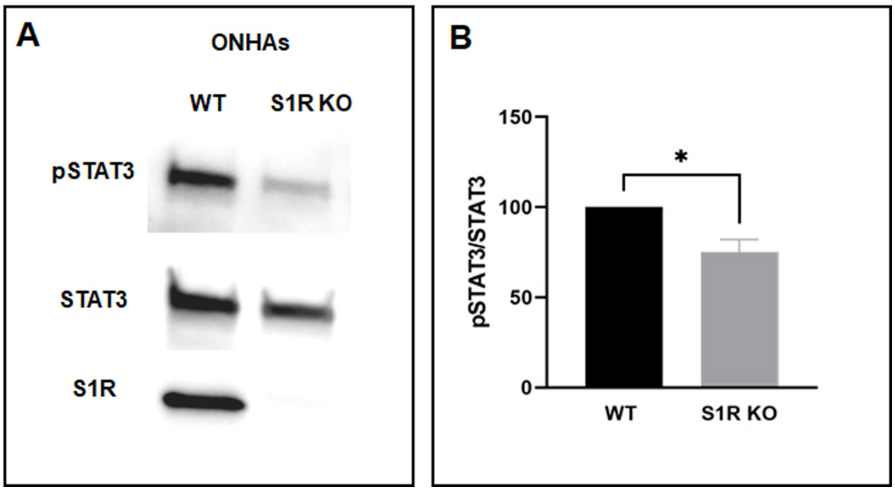

Figure 8. pSTAT3 and STAT3 expression in WT or S1R KO ONHAs cells. (**A**) Representative Western blot showing decreased phosphorylation of STAT3 in S1R KO ONHAs compare to WT ONHAs. (**B**) Quantitative analysis by ImageJ. Significantly different from control at *$P < 0.05$. Data were analyzed using the Student t test. These experiments were repeated in triplicate with cells isolated from different dates, different animals.

conditioned by the ONHAs for 24 hours. The freshly isolated WT RGCs were then plated on coverslips in either RGC whole growth medium or with conditioned medium derived from WT or S1R KO ONHAs. One-half of the medium was changed and replaced with corresponding medium every other day for 7 days. A TUNEL assay was then used to evaluate RGC apoptosis (Fig. 7A). Results were similar to those observed for TUNEL evaluation of indirect ONHA–RGC cocultures (Fig. 6A–B). Quantification of TUNEL-positive cells showed a significant decrease in cellular apoptosis when WT RGCs were incubated with conditioned medium derived from either WT or S1R KO ONHAs (Fig. 7B). In addition, a comparison between groups showed a significant increase in TUNEL positivity when RGCs were cultured with S1R KO ONHA-derived conditioned medium compared with WT ONHA-derived conditioned medium (Fig. 7B). This finding indicates that factors present in the medium derived from ONHAs can protect cultured RGCs from apoptosis, independent of any communication between RGCs and ONHAs in indirect coculture. Furthermore, the lack of S1R within ONHAs causes medium derived from these cells to provide less protection against WT RGC apoptosis than medium derived from WT ONHAs.

Our previous work showed that S1R mediates aspects of ONHA reactivity, and studies indicate that modulation of astrocyte reactivity responses can contribute to neuroprotection, in vitro and in vivo.[28,34,38,41] We previously found that treatment of ONHAs with an S1R agonist enhanced phosphorylation of the signaling molecule, signal transducer and activator of transcription 3 (STAT3), a critical astrocyte reactivity regulator.[41] To evaluate whether presence or absence of S1R in ONHAs affected levels phosphorylated STAT3 (pSTAT3), we prepared cellular lysates from WT versus S1R KO ONHA cultures. Lysates were analyzed by Western blot and probed with antibodies to STAT3 and pSTAT3 (Fig. 8A). Results showed significantly higher levels of pSTAT3 in lysates derived from WT ONHAs compared with lysates derived from S1R KO ONHAs (Figs. 8A and B).

Investigative Ophthalmology & Visual Science

Discussion

We report here the use of a novel ex vivo indirect coculture method to evaluate ONHA-RGC interactions in the presence and absence of S1R. Results of our investigations indicate that, in vitro, the loss of S1R within ONHAs decreases the ability of these cells to support healthy growth and prevent apoptosis of RGCs. Ligands for S1R are in clinical development for a wide range of disorders including neurodegenerative diseases, cancer, drug abuse, and viral infection owing to severe acute respiratory syndrome coronavirus 2.[47–53] Furthermore, stimulation of S1R may offer a useful treatment strategy for optic neuropathies, including glaucoma.[54] Within the optic nerve head, S1R is expressed in both RGCs and astrocytes.[10,11] Therefore, the effects of S1R on RGC–astrocyte interaction are critically important for evaluation of this protein as a therapeutic target.

Historically, the isolation and culture of purified RGCs alone yields lower viability and neurite outgrowth than RGCs in glia-mediated coculture.[55,56] Our results are consistent with this paradigm. Our cell culture model used an indirect coculture technique previously published for combined primary culture of Müller glia and RGCs that showed Müller glia-mediated RGC protection.[44] In addition, studies indicate that cerebral cortex-derived astrocytes significantly extend viability and promote neurite outgrowth when in coculture with RGCs.[55,56] Interestingly, additional previous studies show that the direct coculture of RGCs over a conditioning layer of optic nerve-derived astrocytes only weakly promotes RGC survival.[39] In contrast with these findings, our studies show that indirect coculture with WT optic nerve head-derived astrocytes robustly protects RGCs from apoptosis and improves measures of neurite outgrowth. The apparent disparity between studies is consistent with recent work describing significant heterogeneity in neurotoxic versus neuroprotective astrocyte properties both in vitro and in vivo.[57–60] These properties depend on multiple factors, including the brain or CNS region from which the astrocytes are derived.[30] Further studies are needed to clarify how astrocytic subtypes are established and the conditions under which glia cells derived from specific regions of the optic nerve contribute to versus detract from RGC survival.

In addition to evaluating RGC–ONHA interactions using indirect coculture, we investigated the effects of astrocyte-secreted factors using conditioned medium derived from our cultured ONHAs. We found that conditioned medium from WT ONHA cultures alone also provided robust protection against apoptosis of WT RGCs in culture (Fig. 7). However, WT RGCs exposed to conditioned medium taken from S1R KO ONHA cultures showed significantly greater apoptosis than WT RGCs exposed to WT ONHA-conditioned medium. These results suggest that, in vitro, S1R plays a role in modulating the astrocyte secretome. Indeed, previous studies show that stimulation of S1R with its high affinity agonist, (+)-PTZ, leads to increased astrocytic release of brain-derived neurotrophic factor, a neurotrophin critical to RGC survival.[61–63] In addition, as a ligand-operated protein localized at the endoplasmic reticulum membrane, S1R has been shown to regulate levels of several other proteins that are processed and transported through the cellular secretory pathway.[64,65] Future studies are needed to clarify the role of S1R in modulation of the cellular secretome under conditions of varying cellular stress and tissue microenvironments.

Our previous studies of ONHAs indicate that the activation of S1R using (+)-PTZ leads to the enhancement of astrocyte reactivity characteristics under conditions of cellular stress.[41] In addition, we found that S1R activation in WT ONHAs leads to an increase in phosphorylation of the astrocyte reactivity regulator, STAT3.[41] In the current studies, we find that cellular lysates derived from S1R KO ONHAs show significantly lower levels of phosphorylated STAT3 compared with lysates derived from WT ONHAs. The role of STAT3 in neurodegenerative diseases is incompletely understood. In some disease contexts, including models of Alzheimer's and multiple sclerosis, inhibiting STAT3 activation in astrocytes leads to neuroprotective effects.[66,67] However, interestingly, in vivo studies indicate that the conditional astrocytic KO of STAT3 within the optic nerve leads to decreased measures of astrocyte reactivity and to an increased loss of RGCs under conditions of glaucomatous stress.[34] Additional studies are needed to determine whether the activation or inhibition of S1R in vivo alters STAT3 levels and whether this correlates with the effects of S1R on RGC survival.

In summary, the present work illustrates the importance of S1R to ONHA-mediated support for neurite outgrowth and survival of RGCs in vitro. Future work will examine the mechanisms by which S1R in ONHAs functions to protect RGCs. This will help us to understand the complex neuroprotective role of S1R in ONHAs.

Acknowledgments

Supported by the National Institutes of Health (KEB:R01EY0 27406 SBS: R01EY028103, and Center core grant for vision research (P30) P30 EY031631), and the American Glaucoma Society.

Disclosure: **J. Zhao**, None; **G.B. Gonsalvez**, None; **B.A. Mysona**, None; **S.B. Smith**, None; **K.E. Bollinger**, None

References

1. Hayashi T, Su TP. Sigma-1 receptor chaperones at the ER-mitochondrion interface regulate Ca(2+) signaling and cell survival. *Cell*. 2007;131:596–610.
2. Hayashi T, Su T. The sigma receptor: evolution of the concept in neuropsychopharmacology. *Curr Neuropharmacol*. 2005;3:267–280.
3. Su TP, Su TC, Nakamura Y, Tsai SY. The sigma-1 receptor as a pluripotent modulator in living systems. *Trends Pharmacol Sci*. 2016;37:262–278.
4. Aishwarya R, Abdullah CS, Morshed M, Remex NS, Bhuiyan MS. Sigmar1's molecular, cellular, and biological functions in regulating cellular pathophysiology. *Front Physiol*. 2021;12:705575.
5. Mori T, Hayashi T, Hayashi E, Su TP. Sigma-1 receptor chaperone at the ER-mitochondrion interface mediates the mitochondrion-ER-nucleus signaling for cellular survival. *PLoS One*. 2013;8:e76941.
6. Smith SB, Wang J, Cui X, Mysona BA, Zhao J, Bollinger KE. Sigma 1 receptor: a novel therapeutic target in retinal disease. *Prog Retin Eye Res*. 2018;67:130–149.
7. Barwick SR, Siddiq MS, Wang J, et al. Sigma 1 receptor co-localizes with NRF2 in retinal photoreceptor cells. *Antioxidants (Basel)*. 2021;10:981.
8. Mavlyutov TA, Duellman T, Kim HT, et al. Sigma-1 receptor expression in the dorsal root ganglion: Reexamination using a highly specific antibody. *Neuroscience*. 2016;331:148–157.

9. Alonso G, Phan V, Guillemain I, et al. Immunocytochemical localization of the sigma(1) receptor in the adult rat central nervous system. *Neuroscience*. 2000;97:155–170.
10. Ola MS, Moore P, El-Sherbeny A, et al. Expression pattern of sigma receptor 1 mRNA and protein in mammalian retina. *Brain Res Mol Brain Res*. 2001;95:86–95.
11. Mavlyutov TA, Epstein M, Guo LW. Subcellular localization of the sigma-1 receptor in retinal neurons - an electron microscopy study. *Sci Rep*. 2015;5:10689.
12. Li L, He S, Liu Y, Yorio T, Ellis DZ. Sigma-1R protects retinal ganglion cells in optic nerve crush model for glaucoma. *Invest Ophthalmol Vis Sci*. 2021;62:17.
13. Mueller BH, 2nd, Park Y, Ma HY, et al. Sigma-1 receptor stimulation protects retinal ganglion cells from ischemia-like insult through the activation of extracellular-signal-regulated kinases 1/2. *Exp Eye Res*. 2014;128:156–169.
14. Martin PM, Ola MS, Agarwal N, Ganapathy V, Smith SB. The sigma receptor ligand (+)-pentazocine prevents apoptotic retinal ganglion cell death induced in vitro by homocysteine and glutamate. *Brain Res Mol Brain Res*. 2004;123:66–75.
15. Mavlyutov TA, Guo LW. Peeking into sigma-1 receptor functions through the retina. *Adv Exp Med Biol*. 2017;964:285–297.
16. Shimazawa M, Sugitani S, Inoue Y, Tsuruma K, Hara H. Effect of a sigma-1 receptor agonist, cutamesine dihydrochloride (SA4503), on photoreceptor cell death against light-induced damage. *Exp Eye Res*. 2015;132:64–72.
17. Wang J, Xiao H, Barwick S, Liu Y, Smith SB. Optimal timing for activation of sigma 1 receptor in the Pde6b(rd10)/J (rd10) mouse model of retinitis pigmentosa. *Exp Eye Res*. 2021;202:108397.
18. Zhao J, Mysona BA, Qureshi A, et al. (+)-Pentazocine reduces NMDA-induced retinal ganglion cell death through a sigmaR1-dependent mechanism. *Invest Ophthalmol Vis Sci*. 2016;57:453–461.
19. Smith SB, Duplantier J, Dun Y, et al. In vivo protection against retinal neurodegeneration by sigma receptor 1 ligand (+)-pentazocine. *Invest Ophthalmol Vis Sci*. 2008;49:4154–4161.
20. Mavlyutov TA, Epstein ML, Verbny YI, et al. Lack of sigma-1 receptor exacerbates ALS progression in mice. *Neuroscience*. 2013;240:129–134.
21. Ha Y, Saul A, Tawfik A, et al. Late-onset inner retinal dysfunction in mice lacking sigma receptor 1 (sigmaR1). *Invest Ophthalmol Vis Sci*. 2011;52:7749–7760.
22. Sabino V, Cottone P, Parylak SL, Steardo L, Zorrilla EP. Sigma-1 receptor knockout mice display a depressive-like phenotype. *Behav Brain Res*. 2009;198:472–476.
23. Sha S, Hong J, Qu WJ, et al. Sex-related neurogenesis decrease in hippocampal dentate gyrus with depressive-like behaviors in sigma-1 receptor knockout mice. *Eur Neuropsychopharmacol*. 2015;25:1275–1286.
24. Maurice T, Strehaiano M, Duhr F, Chevallier N. Amyloid toxicity is enhanced after pharmacological or genetic invalidation of the sigma1 receptor. *Behav Brain Res*. 2018;339:1–10.
25. Hong J, Wang L, Zhang T, Zhang B, Chen L. Sigma-1 receptor knockout increases alpha-synuclein aggregation and phosphorylation with loss of dopaminergic neurons in substantia nigra. *Neurobiol Aging*. 2017;59:171–183.
26. Dun Y, Thangaraju M, Prasad P, Ganapathy V, Smith SB. Prevention of excitotoxicity in primary retinal ganglion cells by (+)-pentazocine, a sigma receptor-1 specific ligand. *Invest Ophthalmol Vis Sci*. 2007;48:4785–4794.
27. Zhao J, Mysona BA, Wang J, Gonsalvez GB, Smith SB, Bollinger KE. Sigma 1 receptor regulates ERK activation and promotes survival of optic nerve head astrocytes. *PLoS One*. 2017;12:e0184421.
28. Liddelow SA, Barres BA. Reactive astrocytes: production, function, and therapeutic potential. *Immunity*. 2017;46:957–967.
29. Sofroniew MV, Vinters HV. Astrocytes: biology and pathology. *Acta Neuropathol*. 2010;119:7–35.
30. Hasel P, Rose IVL, Sadick JS, Kim RD, Liddelow SA. Neuroinflammatory astrocyte subtypes in the mouse brain. *Nat Neurosci*. 2021;24:1475–1487.
31. Zamanian JL, Xu L, Foo LC, et al. Genomic analysis of reactive astrogliosis. *J Neurosci*. 2012;32:6391–6410.
32. Karimi-Abdolrezaee S, Billakanti R. Reactive astrogliosis after spinal cord injury-beneficial and detrimental effects. *Mol Neurobiol*. 2012;46:251–264.
33. Johnson EC, Morrison JC. Friend or foe? Resolving the impact of glial responses in glaucoma. *J Glaucoma*. 2009;18:341–353.
34. Sun D, Moore S, Jakobs TC. Optic nerve astrocyte reactivity protects function in experimental glaucoma and other nerve injuries. *J Exp Med*. 2017;214:1411–1430.
35. Wang R, Seifert P, Jakobs TC. Astrocytes in the optic nerve head of glaucomatous mice display a characteristic reactive phenotype. *Invest Ophthalmol Vis Sci*. 2017;58:924–932.
36. Tehrani S, Davis L, Cepurna WO, et al. Astrocyte structural and molecular response to elevated intraocular pressure occurs rapidly and precedes axonal tubulin rearrangement within the optic nerve head in a rat model. *PLoS One*. 2016;11:e0167364.
37. Tehrani S, Davis L, Cepurna WO, et al. Optic nerve head astrocytes display axon-dependent and -independent reactivity in response to acutely elevated intraocular pressure. *Invest Ophthalmol Vis Sci*. 2019;60:312–321.
38. Liddelow SA, Guttenplan KA, Clarke LE, et al. Neurotoxic reactive astrocytes are induced by activated microglia. *Nature*. 2017;541:481–487.
39. Meyer-Franke A, Kaplan MR, Pfrieger FW, Barres BA. Characterization of the signaling interactions that promote the survival and growth of developing retinal ganglion cells in culture. *Neuron*. 1995;15:805–819.
40. Wang J, Shanmugam A, Markand S, Zorrilla E, Ganapathy V, Smith SB. Sigma 1 receptor regulates the oxidative stress response in primary retinal Muller glial cells via NRF2 signaling and system xc(-), the Na(+)-independent glutamate-cystine exchanger. *Free Radic Biol Med*. 2015;86:25–36.
41. Zhao J, Gonsalvez G, Bartoli M, Mysona BA, Smith SB, Bollinger KE. Sigma 1 receptor modulates optic nerve head astrocyte reactivity. *Invest Ophthalmol Vis Sci*. 2021;62:5.
42. Dun Y, Mysona B, Van Ells T, et al. Expression of the cystine-glutamate exchanger (xc-) in retinal ganglion cells and regulation by nitric oxide and oxidative stress. *Cell Tissue Res*. 2006;324:189–202.
43. Winzeler A, Wang JT. Purification and culture of retinal ganglion cells from rodents. *Cold Spring Harb Protoc*. 2013;2013:643–652.
44. Navneet S, Cui X, Zhao J, et al. Excess homocysteine upregulates the NRF2-antioxidant pathway in retinal Muller glial cells. *Exp Eye Res*. 2019;178:228–237.
45. Arshadi C, Gunther U, Eddison M, Harrington KIS, Ferreira TA. SNT: a unifying toolbox for quantification of neuronal anatomy. *Nat Methods*. 2021;18:374–377.
46. Ola MS, Moore P, Maddox D, et al. Analysis of sigma receptor (sigmaR1) expression in retinal ganglion cells cultured under hyperglycemic conditions and in diabetic mice. *Brain Res Mol Brain Res*. 2002;107:97–107.
47. Mavlyutov TA, Guo LW, Epstein ML, Ruoho AE. Role of the sigma-1 receptor in amyotrophic lateral sclerosis (ALS). *J Pharmacol Sci*. 2015;127:10–16.

Investigative Ophthalmology & Visual Science

48. Nguyen L, Lucke-Wold BP, Mookerjee SA, et al. Role of sigma-1 receptors in neurodegenerative diseases. *J Pharmacol Sci*. 2015;127:17–29.
49. Das D, Persaud L, Dejoie J, et al. Tumor necrosis factor-related apoptosis-inducing ligand (TRAIL) activates caspases in human prostate cancer cells through sigma 1 receptor. *Biochem Biophys Res Commun*. 2016;470:319–323.
50. Happy M, Dejoie J, Zajac CK, et al. Sigma 1 receptor antagonist potentiates the anti-cancer effect of p53 by regulating ER stress, ROS production, Bax levels, and caspase-3 activation. *Biochem Biophys Res Commun*. 2015;456:683–688.
51. Gordon DE, Jang GM, Bouhaddou M, et al. A SARS-CoV-2 protein interaction map reveals targets for drug repurposing. *Nature*. 2020;583:459–468.
52. Vela JM. Repurposing sigma-1 receptor ligands for COVID-19 therapy? *Front Pharmacol*. 2020;11:582310.
53. Sambo DO, Lin M, Owens A, et al. The sigma-1 receptor modulates methamphetamine dysregulation of dopamine neurotransmission. *Nat Commun*. 2017;8:2228.
54. Mysona BA, Zhao J, Bollinger KE. Role of BDNF/TrkB pathway in the visual system: therapeutic implications for glaucoma. *Exp Rev Ophthalmol*. 2017;12:69–81.
55. Takahashi N, Cummins D, Caprioli J. Rat retinal ganglion cells in culture. *Exp Eye Res*. 1991;53:565–572.
56. Morgan J, Caprioli J, Koseki Y. Nitric oxide mediates excitotoxic and anoxic damage in rat retinal ganglion cells cocultured with astroglia. *Arch Ophthalmol*. 1999;117:1524–1529.
57. Colombo E, Farina C. Astrocytes: key regulators of neuroinflammation. *Trends Immunol*. 2016;37:608–620.
58. Anderson MA, Burda JE, Ren Y, et al. Astrocyte scar formation aids central nervous system axon regeneration. *Nature*. 2016;532:195–200.
59. Furman JL, Sama DM, Gant JC, et al. Targeting astrocytes ameliorates neurologic changes in a mouse model of Alzheimer's disease. *J Neurosci*. 2012;32:16129–16140.
60. Escartin C, Galea E, Lakatos A, et al. Reactive astrocyte nomenclature, definitions, and future directions. *Nat Neurosci*. 2021;24:312–325.
61. Mysona BA, Zhao J, Smith S, Bollinger KE. Relationship between sigma-1 receptor and BDNF in the visual system. *Exp Eye Res*. 2018;167:25–30.
62. Kikuchi-Utsumi K, Nakaki T. Chronic treatment with a selective ligand for the sigma-1 receptor chaperone, SA4503, up-regulates BDNF protein levels in the rat hippocampus. *Neurosci Lett*. 2008;440:19–22.
63. Ring RM, Regan CM. Captodiamine, a putative antidepressant, enhances hypothalamic BDNF expression in vivo by synergistic 5-HT2c receptor antagonism and sigma-1 receptor agonism. *J Psychopharmacol*. 2013;27:930–939.
64. Maher CM, Thomas JD, Haas DA, et al. Small-molecule sigma1 modulator induces autophagic degradation of PD-L1. *Mol Cancer Res*. 2018;16:243–255.
65. Lopez OV, Gorantla S, Segarra AC, et al. Sigma-1 receptor antagonist (BD1047) decreases cathepsin B secretion in HIV-infected macrophages exposed to cocaine. *J Neuroimmune Pharmacol*. 2019;14:226–240.
66. Qin H, Yeh WI, De Sarno P, et al. Signal transducer and activator of transcription-3/suppressor of cytokine signaling-3 (STAT3/SOCS3) axis in myeloid cells regulates neuroinflammation. *Proc Natl Acad Sci USA*. 2012;109:5004–5009.
67. Reichenbach N, Delekate A, Plescher M, et al. Inhibition of Stat3-mediated astrogliosis ameliorates pathology in an Alzheimer's disease model. *EMBO Mol Med*. 2019;11:e9665.